Author Manuscript

Author Manuscript

Author Manuscript

Author Manuscript

HHS Public Access

Author manuscript

J Control Release. Author manuscript; available in PMC 2016 December 28.

Published in final edited form as:

J Control Release. 2015 December 28; 220(0 0): 61–70. doi:10.1016/j.jconrel.2015.10.004.

Detection of Atherosclerotic Lesions and Intimal Macrophages Using CD36-Targeted Nanovesicles

Shufang Nie[1,†], **Jia Zhang**[1,†], **Raul Martinez-Zaguilan**[2], **Souad Sennoune**[2], **Md Nazir Hossen**[1], **Alice H. Lichtenstein**[3], **Jun Cao**[1,4], **Gary E. Meyerrose**[5], **Ralph Paone**[6], **Suthipong Soontrapa**[5], **Zhaoyang Fan**[7], and **Shu Wang**[1,*]

[1]Department of Nutritional Sciences, Texas Tech University, Lubbock, TX 79409, USA

[2]Department of Cell Physiology and Molecular Biophysics, Texas Tech University Health Sciences Center, Lubbock, TX 79416, USA

[3]Cardiovascular Nutrition Laboratory, Jean Mayer Human Nutrition Research Center on Aging, Tufts University, Boston, MA 02111, USA

[4]State Key Laboratory of Food Science and Technology, Nanchang University, Nanchang 330047, Jiangxi, China

[5]Division of cardiology, Department of Internal Medicine, Texas Tech University Health Sciences Center, Lubbock, TX 79430, USA

[6]Department of Surgery, Texas Tech University Health Sciences Center, Lubbock, TX 79430, USA

[7]Department of Electrical and Computer Engineering and Nano Tech Center, Texas Tech University, Lubbock, TX 79409, USA

Abstract

Current approaches to the diagnosis and therapy of atherosclerosis cannot target to lesion-determinant cells in the artery wall. Intimal macrophage infiltration promotes atherosclerotic lesion development by facilitating the accumulation of oxidized low-density lipoproteins (oxLDL) and increasing inflammatory responses. The presence of these cells is positively associated with lesion progression, severity and destabilization. Hence, they are an important diagnostic and therapeutic target. The objective of this study was to noninvasively assess the distribution and accumulation of intimal macrophages using CD36-targeted nanovesicles. Soy phosphatidylcholine was used to synthesize liposome-like nanovesicles. 1-(Palmitoyl)-2-(5-keto-6-octene-dioyl) phosphatidylcholine was incorporated on their surface to target the CD36 receptor. All *in vitro* data demonstrate that these targeted nanovesicles had a high binding affinity for the oxLDL binding site of the CD36 receptor and participated in CD36-mediated recognition and uptake of

[*]To whom correspondence should be addressed: Dr. Shu Wang, Department of Nutritional Sciences, Texas Tech University, 1301 Akron Avenue, Lubbock, TX 79409-1270, USA, Telephone number: (806) 834-4050, shu.wang@ttu.edu.
[†]Both authors contributed equally to this study and share first authorship

Publisher's Disclaimer: This is a PDF file of an unedited manuscript that has been accepted for publication. As a service to our customers we are providing this early version of the manuscript. The manuscript will undergo copyediting, typesetting, and review of the resulting proof before it is published in its final citable form. Please note that during the production process errors may be discovered which could affect the content, and all legal disclaimers that apply to the journal pertain.

Author Manuscript Author Manuscript Author Manuscript Author Manuscript

nanovesicles by macrophages. Intravenous administration into LDL receptor null mice of targeted compared to non-targeted nanovesicles resulted in higher uptake in aortic lesions. The nanovesicles co-localized with macrophages and their CD36 receptors in aortic lesions. This molecular target approach may facilitate the *in vivo* noninvasive imaging of atherosclerotic lesions in terms of intimal macrophages accumulation and distribution and disclose lesion features related to inflammation and possibly vulnerability thereby facilitate early lesion detection and targeted delivery of therapeutic compounds to intimal macrophages.

Graphical abstract

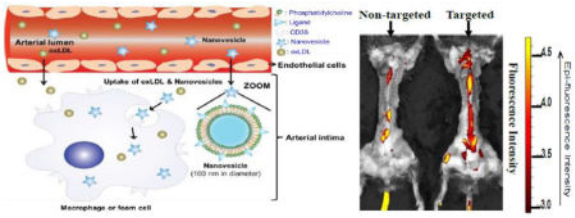

Illustration of CD36-targeted nanovesicle composition, structure and targeting mechanisms to intimal macrophages and images showing their target specificity to aortic lesions in LDLr−/− mice

Keywords

Atherosclerosis; CD36; Macrophages; Oxidized lipids; Nanovesicles; Targeted delivery

1. Introduction

Atherosclerotic cardiovascular disease is the leading cause of mortality in the United States. Macrophages play an important role in lesion initiation and progression by facilitating cholesterol accumulation and promoting an inflammatory response [1, 2]. This disease is sometimes referred to as the silent killer because it is characterized by the absence of symptomology until relatively severe vessel occlusion occurs. Current detection techniques, such as ultrasound, magnetic resonance imaging and computed tomography, cannot effectively detect atherosclerotic lesions at the cellular level and disclose lesion features [3–5].

Macrophages are signature cells of atherosclerotic lesions. Recruitment and infiltration of monocytes into the arterial wall and subsequent conversion to macrophages are the precursor of atherosclerotic lesion development [6]. Accumulation of intimal macrophages positively correlates with lesion size [7–9]. In addition, intimal macrophages destabilize the surface of the lesion [4, 7–10]. Therefore, targeting intimal macrophages is a promising avenue for characterizing atherosclerotic lesions and inflammatory state [11].

Macrophages take up modified low-density lipoproteins (LDL) via scavenger receptors, particularly the CD36 receptor [1]. Uptake of modified LDL by macrophages can be as high as 20 times that of native LDL [12, 13]. The predominant form of modified LDL in humans is oxidized LDL (oxLDL). CD36-null mice have a 70% or greater reduction in aortic lesion size, and peritoneal macrophages isolated from these mice exhibit a 60–80% lower oxLDL

Author Manuscript Author Manuscript Author Manuscript Author Manuscript

binding and uptake rates [14]. These data demonstrate the critical role of the macrophage CD36 receptor in cholesterol accumulation and lesion progression [15, 16]. OxLDL particles have oxidized phosphatidylcholine (PC) on their surface. Oxidized PC has been detected in atherosclerotic lesions and is thought to be a ligand for binding of oxLDL to the macrophage CD36 receptor [16–19]. CD36 receptor expression correlates with lesion severity [15, 16, 20]. Therefore, targeting the macrophage CD36 receptor is a promising approach to detect atherosclerotic lesions [21–24]. 1-(Palmitoyl)-2-(5-keto-6-octene-dioyl)PC (KOdiA-PC), a type of oxidized PC found on oxLDL, has a high binding affinity to the CD36 receptor and participates in CD36-mediated recognition and uptake of particles by intimal macrophages [25]. However, intimal macrophage targeting specificity of KOdiA-PC in atherosclerosis animal models was not reported. To our knowledge, this is the first study to investigate whether nanovesicles carrying KOdiA-PC on their surface can target to atherosclerotic lesions via binding to intimal macrophages in LDLr−/− mice.

Nanomedicine is promising in developing novel diagnostic and therapeutic agents, and therefore has gained tremendous attention in biomedical research [26]. Nanovesicles can enhance solubility, stability and payload of diagnostic agents, preventive compounds and therapeutic drugs, and enhance their absorption and bioavailability through protecting them from premature degradation and prolonging their circulation time. They can exhibit high differential uptake efficiency in the target cells (or tissues) over normal cells (or tissue) through passive or active target strategies, lower toxicity through preventing them from prematurely interacting with the biological environment [27]. When an atherosclerotic lesion is developing, the permeability of the endothelial layer is enhanced, allowing for the accelerated influx of lipoproteins and small particles such as nanovesicles to migrate into the intimal layer [28]. Expanding atherosclerotic lesions requires oxygen and nutrients, promoting neoangiogenesis [29]. These neovessels are prone to be leaky and fragile resulting in enhanced permeability and retention, further promoting migration of nanovesicles into the lesion area [30].

The aim of this work was to assess the feasibility of detecting atherosclerotic lesions by forming liposome-like nanovesicles with KOdiA-PC on the surface and assessing their target specificity to intimal macrophages, particularly through CD36 receptors (Fig. 1). Our hypothesis was that the targeted nanovesicles would accumulate in atherosclerotic lesions through binding to CD36 receptors on intimal macrophages and thereby facilitate the identification of atherosclerotic lesions and further define the biological features of the lesions, particularly distribution and accumulation of intimal macrophages. This study has a potential clinical application for targeted delivery of anti-atherogenic drugs and diagnostic agents to intimal macrophages in lesions.

2. Material and methods

2.1. Nanovesicle preparation

Stock solution composed of 2.6 mmol/L soy PC (>95%, Avanti Polar Lipids) with (targeted nanovesicles) or without (non-targeted nanovesicles) KOdiA-PC (Cayman Chemical) were prepared in 1xPBS by extrusion (10 times each filter) through 0.2 μm then 0.05 μm polycarbonate filters using an Avanti Mini-Extruder Set (Avanti Polar Lipids). KOdiA-PC

Author Manuscript Author Manuscript Author Manuscript Author Manuscript

replaced 30% in moles of soy PC. For *in vitro* binding and uptake experiments, 7-nitro-2-1, 3-benzoxadiazol-4-yl-phosphatidylcholine (NBD-PC, 2 mol%) was incorporated into nanovesicles. The size and polydispersity index of nanovesicles were measured using a Brookhaven BI-MAS particle size analyzer. The zeta potential of nanovesicles was measured using a Brookhaven ZetaPALS analyzer. The size and morphology of nanovesicles were measured and confirmed using a Hitachi 8100 transmission electron microscope (TEM).

2.2. Nanovesicle *in vitro* binding and uptake

2.2.1. Elicited peritoneal macrophage isolation and culture—Male C57B6/J mice from the Jackson Laboratory at age 8–12 weeks were used for collecting elicited peritoneal macrophages as previously described [31].

2.2.2. CD36 knockdown in elicited mouse peritoneal macrophages—Mouse elicited peritoneal macrophages were transfected without or with CD36 siRNA or scramble siRNA using Lipofectamine® RNAiMAX Transfection Reagent (Life Technologies) for 24 and 48 hours. Thereafter macrophages CD36 mRNA and protein levels were measured using real-time PCR and an immunostaining method, respectively. RNA isolation, reverse transcription and real-time PCR were conducted as previously described [31]. Beta (β)-actin was used as endogenous control. CD36 forward primer: ATTAATGGCACAGACGCAGC; CD36 reverse primer: CCGAACACAGCGTAGATAGACC; β-actin forward primer: CTTTTCCAGCCTTCCTTCTTGG; β-actin reverse primer: CAGCACTGTGTTGGCATAGAGG. For measuring CD36 protein expression, macrophages were washed with 1×PBS and fixed with ice cold methanol for 10 minutes. After incubation with 1% bovine serum albumin (BSA) for 1 hour at room temperature, the macrophages were stained with RPE-conjugated rat anti-mouse CD36 antibody (1:200) overnight at 4°C in the dark. Cell nuclei were stained with DAPI and then visualized under an EvoS Auto fluorescence microscope.

2.2.3. THP-1 culture and differentiation—Human monocytic THP-1 cells (American Type Culture Collection) were cultured in RPMI 1640 containing 10% of FBS. Cell differentiation was induced by incubating 5×10^5 cells/mL with 1.6 nmol/L phorbol 12-myristate 13-acetate (Sigma-Aldrich, St. Louis, MO) for 72 hours.

2.2.4. Human LDL isolation and minimally oxLDL preparation—LDL was isolated from human plasma by a sequential ultracentrifugation method [32]. Minimally oxidized LDL was prepared by exposing human LDL to 2 μM $CuSO_4$ for 5 hours and oxidation was confirmed by measuring thiobarbituric acid-reactive substances [33].

2.2.5. Binding and uptake of nanovesicles by macrophages—(i) Normal binding and uptake assay. Mouse elicited peritoneal macrophages, THP-1 derived macrophages were treated with NBD-labeled non-targeted or targeted nanovesicles. After confirming CD36 mRNA and protein expression, CD36 knockdown or CD36 negative control (scrambled siRNA) or control (no siRNA treatment) mouse elicited peritoneal macrophages were treated with NBD-labeled non-targeted or targeted nanovesicles for 2 hours at 37°C. (ii)

Author Manuscript Author Manuscript Author Manuscript Author Manuscript

Competitive binding assay with mouse CD36 antibody. Mouse elicited peritoneal macrophages were treated with RPE-labeled anti-CD36 antibody (MCA2748PE, AbD Serotec) in combination with NBD-labeled non-targeted or targeted nanovesicles for 2 hours at 4°C. (iii) Competitive binding assay with human minimally oxLDL. THP-1 derived macrophages were treated with 40 μg protein/mL of human minimally oxLDL in combination with NBD-labeled non-targeted or targeted nanovesicles for 2 hours at 37°C.

After incubation, cells were then washed three times with ice cold 1xPBS (pH 7.4) and fixed with 3.7% formaldehyde in 1xPBS (pH 7.4) for 10 minutes at room temperature. After washing with ice cold 1xPBS (pH 7.4) three times, nuclei were stained with DAPI solution (IHC World, LLC.) for 10 minutes at room temperature in the dark. Cells were washed again with ice cold 1xPBS (pH 7.4) and visualized under an EvoS Auto fluorescence microscope. Microscopy settings were identical for all measures to allow equal comparison of the images.

2.2.6. Cellular cholesterol content—THP-1 derived macrophages were pre-treated with non-targeted or targeted nanovesicles for 30 minutes at 37°C. Then cells were further incubated with 40 μg protein/mL of human minimally oxLDL for additional 1.5 hours at 37°C. After washing the cells three times with 1xPBS, cells were collected for protein and cholesterol measurement. Macrophage lipids were extracted overnight using a chloroform/methanol (2:1, v/v) mixture. Macrophage TC and FC were determined using a high performance liquid chromatography (HPLC) system (Waters Co., Milford, MA) with a C18 reverse-phase column (150 mm×4.6 mm, 5 μm size) and a Waters 2489 UV/Visible detector as previously described [34]. CE was calculated as the difference between TC and FC. Macrophages were digested in 0.5N NaOH and total protein was determined using a bicinchoninic acid (BCA) kit (Pierce Ins., Rockford, IL). Macrophage cholesterol concentrations were expressed as μmol of cholesterol per g of protein.

2.3. *In vivo* targeting of nanovesicles to atherosclerotic lesions

2.3.1. Animals and diet—Eight male 6-week old LDLr−/− mice with C57BL6 background (from the Jackson Laboratory) were fed an atherogenic diet (Harlan Teklad, TD. 88137) containing 21% of saturated fat (w/w) and 0.15% of cholesterol (w/w) for about 25 weeks. C57BL6 mice were used as non-lesion control mice. Mice were housed at 22 to 24°C, 45% relative humidity and a daily 12/12 light/dark cycle with the light period from 07:00 to 19:00. Food and water were given ad libitum. Body weights of mice at the time of experiments ranged from 40–45 g. Based on the body weight, all LDLr−/− mice and C57BL6 mice were grouped before receiving treatments. The animal protocol was approved by the animal care and use committee of Texas Tech University, Lubbock, TX.

2.3.2. In vivo imaging of atherosclerosis and immunohistochemistry—For *in vivo* imaging experiments, 1,1′-dioctadecyl-3,3,3′,3′-tetramethyl indotricarbocyanine iodide (DiR), a near infrared fluorescence dye (λ of excitation is 730 nm, λ of emission is 790 nm), replaced 2 mol% of soy PC. Incorporated DiR amounts in both targeted and non-targeted nanovesicle were measured using a Shimadzu UV-3600 UV-VIS-NIR Spectrophotometer. Non-targeted nanovesicles and targeted nanovesicles containing the same amounts of DiR

Author Manuscript Author Manuscript Author Manuscript Author Manuscript

were intravenously injected into mice via tail veins. After 20-hour injection, mice were imaged using an IVIS® Lumina XR imaging system (Caliper Life Science) with a near infrared filter (λ of excitation is 745 nm, λ of emission is 800 nm). Mice were then sacrificed and their hearts were perfused with 1xPBS through the left ventricle. After removing liver, spleen, kidneys, and additional abdominal organs and tissues, the fluorescence reflectance images of aortas were acquired *in situ* and after dissection using the IVIS® Lumina XR imaging system (Caliper Life Science). The aortas were also visualized under the EvoS Auto fluorescence microscope with a Cy7 filter (λ of excitation is 710/40, λ of emission is 775/46). Subsequently, the dissected aortas were embedded in Tissue-Tek O.C.T. (Sakura), snap-frozen in liquid nitrogen, and serially sectioned about 600 slides (5 μm thick) from each aorta. The DiR (nanovesicles) signals were observed every 10 slides using the EvoS Auto fluorescence microscope with the Cy7 filter. We also stained the adjacent slides using Oil red O to identify the lesions. After fixed with cold acetone, adjacent cross-sections of aortas were immunostained with RPE-conjugated rat anti-mouse CD36 antibody, or with F4/80 antibody (sc-52664, Santa Cruz Biotechnology) at 4°C overnight and then the secondary antibody Cy3-conjugated AffiniPure Donkey Anti-Rat IgG was used for F4/80 detection. The secondary antibody was incubated with cross-sections of aortas for an additional 4 hours at ambient temperature. After washing, the cross-sections of aortas were mounted with ProLong® Gold Antifade Reagent containing DAPI (P-36931, Life technologies) for 1 hour at ambient temperature, and then sections were visualized under the EvoS Auto fluorescence microscope.

2.4. Statistics

Data of macrophage cholesterol content and nanovesicle signals in the cross-sections of atherosclerotic lesions were statistically analyzed by 2-tailed paired student's t test using the SPSS software (version 18.0; SPSS Inc, Chicago, IL). Differences were considered significant at $p<0.05$. Data are presented in Figures and table as means ± standard deviation.

3. Results

3.1. Characteristics of nanovesicles

The nanovesicles had a mean particle diameter of 100 nm and mean polydispersity index of 0.10 as measured using a Brookhaven BI-MAS particle size analyzer (Table 1). The zeta potential of the nanovesicles was about −22 mV measured using a Brookhaven ZetaPALS analyzer (Table 1). The nanovesicle size was confirmed using transmission electron microscope (TEM) measurements. TEM images indicated that nanovesicles had a quasi-spherical shape (Fig. 2).

3.2. Targeted nanovesicles bound to mouse macrophages via CD36

NBD-labeled targeted nanovesicles had a higher binding affinity to and uptake by mouse peritoneal macrophages than NBD-labeled non-targeted nanovesicles (Fig. 3A). Co-incubation of targeted nanovesicles with a CD36 antibody dramatically decreased their binding affinity to mouse peritoneal macrophages (Fig. 3B). CD36 siRNA transfection decreased mouse peritoneal macrophage CD36 mRNA levels by 56% and 82% after incubation for 24 and 48 hours, respectively. CD36 protein levels were reduced by about

Author Manuscript Author Manuscript Author Manuscript Author Manuscript

80% after 48-hour of CD36 siRNA transfection (Fig. 3C). Scramble siRNA transfection did not significantly change CD36 expression. CD36 knockdown macrophages bound and took up less NBD-labeled targeted nanovesicles than control or CD36 negative control macrophages (Fig. 3D).

3.3. Targeted nanovesicles bound to human macrophages via CD36

NBD-labeled targeted nanovesicles had higher binding affinity to and uptake by human THP-1 derived macrophages than NBD-labeled non-targeted nanovesicles (Fig. 4A). Co-incubation of targeted nanovesicles with human minimally oxLDL significantly decreased their binding and uptake by human macrophages (Fig. 4B). The binding and uptake of non-targeted nanovesicles by human THP-1 derived macrophages were extremely low, regardless of the presence or absence of oxLDL (Fig. 4A&B). Human THP-1 derived macrophages expressed high levels of CD36 receptors (Fig. 4C).

3.4. Targeted nanovesicles decreased macrophage cholesterol content

Targeted compared to non-targeted nanovesicles significantly decreased total cholesterol (TC) and free cholesterol (FC) content, but not cholesteryl ester (CE) content, in human THP-1 derived macrophages when co-incubated with human minimally oxLDL (Fig. 4D).

3.5. Targeted nanovesicles detected atherosclerotic lesions in LDL receptor null (LDLr−/−) mice

We selected the 20-hour post-injection time point based on published studies [35–37] and particularly our pilot study. After tail vein injection of DiR-labelled non-targeted or targeted nanovesicles to mice, much more targeted than non-targeted nanovesicles was distributed in the liver, heart, aorta and other central organs after short post-injection time. This difference was maintained pretty long to 20-hour post-injection. Although a short waiting time will give more positive results and also is more convenient from the clinical diagnostic perspective, we selected the more conservative 20-h post-injection for our rest experiments in this study. Additionally, 20-hour post-injection allows us to investigate the prolonged target effect of nanovesicles.

After twenty hours of post-intravenous injection of DiR-labeled nanovesicles into C57BL6J mice without lesions and LDLr−/− mice with lesions, the aortas were imaged using an IVIS® Lumina XR imaging system. The higher DiR intensity indicates a higher target level of the nanovesicles (Fig. 5). Both DiR-labeled non-targeted and targeted nanovesicles did not target to aortas (no lesions) in C57BL6J control mice (Fig. 5A). However, targeted compared to non-targeted nanovesicles had higher target specificity to the aortas with lesions in LDLr−/− mice (Fig. 5B&C) and had a stronger signal in the lesion areas as visualized on the longitudinally opened aortas isolated from those mice (Fig. 5D). The results were consistent for all 4 pairs of LDLr−/− mice having atherosclerotic lesions. Targeted nanovesicles had higher target specificity to the atherosclerotic lesions on cross-sections of aortas isolated from LDLr−/− mice than non-targeted nanovesicles (Fig. 6A-a & 6A-b-1). There was no evidence of non-specific binding of targeted nanovesicles to aortas without lesions isolated from C57BL6J mice (Fig. 6A-b-2). We analyzed DiR (nanovesicle) signals in the cross-sections of aortic lesions using the NIH Image J software. The targeted

Author Manuscript Author Manuscript Author Manuscript Author Manuscript

nanovesicles had more than 2-fold higher intensity in the lesion areas than non-targeted nanovesicles ($p<0.05$) (Fig. 6B).

3.6. Targeted nanovesicles identified intimal macrophages via CD36 receptors

Cross-sections of aortas were stained with Oil red O and immunohistochemistry was used to identify macrophages and CD36 receptors in adjacent slides. The majority of targeted nanovesicles were detected in the lesion cap or shoulder area (Fig. 7). The targeted nanovesicles co-localized with macrophages (F4/80) and CD36 receptors, indicating that these nanovesicles targeted the intimal macrophages via binding to CD36 receptors (Fig. 7).

4. Discussion

We have successfully synthesized liposome-like nanovesicles, which carry KOdiA-PC on their surface and can target macrophages via binding to their CD36 receptors. The targeted nanovesicles detected not only the lesion location and area, but also macrophage distribution and accumulation in the arterial wall. Macrophages are determinant cells in arterial lesion formation and progression, and characterize lesion vulnerability [38–40]. Accumulation of intimal macrophages positively correlates with lesion size and area [7–9]. Macrophage-dense inflammation, especially in the shoulder and cap regions, large lipid cores, and thin fibrous caps are major characteristics of vulnerable lesions [4, 41–43]. The CD36-targeted nanovesicles accurately identified not only the lesion area and size, but also macrophage distribution and accumulation, and could provide important information for lesion vulnerability. In the LDLr−/− mouse model used in this study, macrophage accumulation was particularly rich in the cap and shoulder areas of the lesions.

The target ligand, KOdiA-PC, has been identified in oxLDL isolated from humans. It has a high binding affinity to CD36-expressing macrophages, especially intimal macrophages [44, 45]. Oxidized PC is found on oxLDL and at high concentrations in atherosclerotic lesions of animals [25, 46]. Therefore, they are strong candidate ligands for oxLDL binding to macrophages. Lesion development and progression increases CD36 expression [15, 16, 20]. Increased CD36-mediated oxLDL uptake by intimal macrophages further upregulates CD36 expression [47]. KOdiA-PC, has been identified in oxLDL and has a high binding affinity to the CD36 receptor [25]. In the current work, when nanovesicles carrying KOdiA-PC were delivered intravenously into LDLr−/− mice, the target specificity to intimal macrophages was strong. These data are consistent with our *in vitro* results. On the surface of oxLDL, hydrophilic head and *sn*-2 acyl group of KOdiA-PC is protruded from the phospholipid membrane into the aqueous phase, resulting in a lipid whisker model [48]. The protruded and oxidized *sn*-2 acyl group that incorporates a terminal γ-hydroxy (or oxo)-α,β-unsaturated carbonyl is essential for its high binding affinity to the macrophage CD36 receptor [19, 25, 48–50]. In the current work we mixed KOdiA-PC with PC to make targeted nanovesicles, whose surface composition and lipid whisker structure should be similar to oxLDL. Their binding affinity to macrophages was then assessed *in vitro* and *in vivo*. The results indicate that targeted nanovesicles have a higher binding affinity to both human and mouse macrophages than non-targeted nanovesicles. Decreased binding affinity of targeted nanovesicles to CD36-knockdown macrophages and to macrophages co-incubating with CD36 antibody or oxLDL indicates that the targeted nanovesicles bind to

Author Manuscript Author Manuscript Author Manuscript Author Manuscript

macrophages via CD36 receptors. The high expression of CD36 receptors in the intimal macrophages enhances their affinity for the targeted nanovesicles carrying KOdiA-PC. These data are consistent with our *in vivo* data indicating that targeted nanovesicle signals co-localize with CD36 receptors and macrophages in the cross-sections of atherosclerotic lesions isolated from LDLr−/− mice. Most importantly, nanovesicle signals are not found in non-lesion areas of LDLr−/− and C57BL6J mice. Therefore, our KOdiA-PC nanovesicles can migrate into the artery wall and target intimal macrophages via binding to their CD36 receptors, which allows for not only the detection of atherosclerotic lesion size, surface area and location, but also the image of the extent of macrophage infiltration and distribution in the lesions.

Nanoparticles have been used to image intimal macrophages and treat atherosclerosis via targeted delivery of therapeutic compounds to intimal macrophages. Ultra-small superparamagnetic iron oxide (USPIO)-enhanced magnetic resonance imaging (MRI) has been widely used to detect intimal macrophages, because of the phagocytotic function of macrophages on most foreigners, like iron oxide particles, in the whole body [39, 51]. However, concerns have risen for the toxicity and accumulation of iron oxide nanoparticles in the body. Incorporation of antibodies on the surface of nanovesicles to target to macrophage scavenger receptors has been investigated, but they may increase immune reactions and response in the body [52]. Synthetic high-density lipoproteins have also been used, but have similar target specificity challenges [53, 54]. Since intimal macrophages and foam cells secrete reactive oxygen species, matrix metalloproteinases, cytokines and chemokines, express a high level of glucose transporters and scavenger receptors, those can be used as potential molecular imaging targets for intimal macrophages and atherosclerotic lesions [4, 55]. Other studies detected atherosclerotic lesions *via* targeting other cells and molecules in the lesions, including endothelial cells, vascular smooth-muscle cells, collagen, natriuretic peptide receptor C (NPR-C) and so on [4, 56–59].

We used PC to make liposome-like nanovesicles and incorporated KOdiA-PC on the surface of nanovesicles. Because these compounds are biocompatible and biodegradable, they should have low levels of side effects or toxicity. KOdiA-PC can be incorporated on the phospholipid membranes of liposomes or other nanovesicles without using conjugation or modification reactions, which are required for conjugating a target peptide or antibody on the surface of nanovesicles. Additionally, KOdiA-PC ligand allowed nanovesicles to stay in the aortic lesions for a prolonged time, which might indicate a more stable and strong affinity to the macrophage CD36 receptor than other small molecule peptides. Our *in vitro* and *in vivo* data clearly indicate that they can target specifically to intimal macrophages *via* binding to CD36 receptors, whose expression correlates with lesion severity. Ultrasound contrast agents, MRI contrast agents, radiotracers, near-infrared fluorescent dyes can be loaded into our targeted nanovesicles, which allow us to image intimal macrophages using intravascular ultrasound, MRI, computed tomography (CT)/CT angiography, positron emission tomography (PET)/single-photon emission CT (SPECT), optical coherence tomography, and other imaging modalities [29, 60–64].

We used LDLr−/− mice with advanced atherosclerotic lesions in this study. Non-human primates, pig or other predictive animal models with different stages of atherosclerotic

Author Manuscript Author Manuscript Author Manuscript Author Manuscript

lesions will be needed in confirming the experimental results in future studies. Additional experiments are required to investigate the pharmacokinetics and pharmacodynamics of the targeted nanovesicles and incorporated compounds before translating it to clinical application. CD36-targeted nanovesicles carrying KOdiA-PC detected not only the lesion location and size, but also lesion macrophage distribution and accumulation, which can reveal lesion characteristics and features. This study opens a door for developing many innovative strategies for diagnosis, prevention and treatment of atherosclerosis.

Supplementary Material

Refer to Web version on PubMed Central for supplementary material.

Acknowledgments

The project described was supported by Grant Number R15AT007013 and 1R15AT008733-01 from the National Center for Complementary and Integrative Health. The content is solely the responsibility of the authors and does not necessarily represent the official views of the National Center for Complementary & Alternative Medicine or the National Institutes of Health. Additional support was provided by the Burleson's Family Foundation and College of Human Sciences at Texas Tech University, Lubbock, TX.

The authors would like to thank Dr. Naima Moustaid-Moussa and Shane Scoggin for their technical support in immunohistochemistry, and Dr. Fazle Hussain for his thoughtful critical review of the manuscript.

References

1. Kunjathoor VV, Febbraio M, Podrez EA, Moore KJ, Andersson L, Koehn S, Rhee JS, Silverstein R, Hoff HF, Freeman MW. Scavenger receptors class A-I/II and CD36 are the principal receptors responsible for the uptake of modified low density lipoprotein leading to lipid loading in macrophages. J Biol Chem. 2002; 277:49982–49988. [PubMed: 12376530]
2. Ludewig B, Laman JD. The in and out of monocytes in atherosclerotic plaques: Balancing inflammation through migration. Proc Natl Acad Sci U S A. 2004; 101:11529–11530. [PubMed: 15292506]
3. Quillard T, Croce K, Jaffer FA, Weissleder R, Libby P. Molecular imaging of macrophage protease activity in cardiovascular inflammation in vivo. Thromb Haemost. 2011; 105:828–836. [PubMed: 21225096]
4. Libby P, DiCarli M, Weissleder R. The vascular biology of atherosclerosis and imaging targets. J Nucl Med. 2010; 51(Suppl 1):33S–37S. [PubMed: 20395349]
5. Camici PG, Rimoldi OE, Gaemperli O, Libby P. Non-invasive anatomic and functional imaging of vascular inflammation and unstable plaque. Eur Heart J. 2012; 33:1309–1317. [PubMed: 22507974]
6. Stoneman V, Braganza D, Figg N, Mercer J, Lang R, Goddard M, Bennett M. Monocyte/macrophage suppression in CD11b diphtheria toxin receptor transgenic mice differentially affects atherogenesis and established plaques. Circ Res. 2007; 100:884–893. [PubMed: 17322176]
7. Weber C, Zernecke A, Libby P. The multifaceted contributions of leukocyte subsets to atherosclerosis: lessons from mouse models. Nat Rev Immunol. 2008; 8:802–815. [PubMed: 18825131]
8. Packard RR, Lichtman AH, Libby P. Innate and adaptive immunity in atherosclerosis. Semin Immunopathol. 2009; 31:5–22. [PubMed: 19449008]
9. Robbins CS, Hilgendorf I, Weber GF, Theurl I, Iwamoto Y, Figueiredo JL, Gorbatov R, Sukhova GK, Gerhardt LM, Smyth D, Zavitz CC, Shikatani EA, Parsons M, van Rooijen N, Lin HY, Husain M, Libby P, Nahrendorf M, Weissleder R, Swirski FK. Local proliferation dominates lesional macrophage accumulation in atherosclerosis. Nat Med. 2013; 19:1166–1172. [PubMed: 23933982]
10. Naghavi M, Libby P, Falk E, Casscells SW, Litovsky S, Rumberger J, Badimon JJ, Stefanadis C, Moreno P, Pasterkamp G, Fayad Z, Stone PH, Waxman S, Raggi P, Madjid M, Zarrabi A, Burke A, Yuan C, Fitzgerald PJ, Siscovick DS, de Korte CL, Aikawa M, Juhani Airaksinen KE,

Author Manuscript Author Manuscript Author Manuscript Author Manuscript

Assmann G, Becker CR, Chesebro JH, Farb A, Galis ZS, Jackson C, Jang IK, Koenig W, Lodder RA, March K, Demirovic J, Navab M, Priori SG, Rekhter MD, Bahr R, Grundy SM, Mehran R, Colombo A, Boerwinkle E, Ballantyne C, Insull W Jr, Schwartz RS, Vogel R, Serruys PW, Hansson GK, Faxon DP, Kaul S, Drexler H, Greenland P, Muller JE, Virmani R, Ridker PM, Zipes DP, Shah PK, Willerson JT. From vulnerable plaque to vulnerable patient: a call for new definitions and risk assessment strategies: Part I. Circulation. 2003; 108:1664–1672. [PubMed: 14530185]

11. Sanz J, Fayad ZA. Imaging of atherosclerotic cardiovascular disease. Nature. 2008; 451:953–957. [PubMed: 18288186]
12. Brown MS, Goldstein JL, Krieger M, Ho YK, Anderson RG. Reversible accumulation of cholesteryl esters in macrophages incubated with acetylated lipoproteins. J Cell Biol. 1979; 82:597–613. [PubMed: 229107]
13. Goldstein JL, Ho YK, Basu SK, Brown MS. Binding site on macrophages that mediates uptake and degradation of acetylated low density lipoprotein, producing massive cholesterol deposition. Proc Natl Acad Sci U S A. 1979; 76:333–337. [PubMed: 218198]
14. Febbraio M, Abumrad NA, Hajjar DP, Sharma K, Cheng W, Pearce SF, Silverstein RL. A null mutation in murine CD36 reveals an important role in fatty acid and lipoprotein metabolism. J Biol Chem. 1999; 274:19055–19062. [PubMed: 10383407]
15. Febbraio M, Podrez EA, Smith JD, Hajjar DP, Hazen SL, Hoff HF, Sharma K, Silverstein RL. Targeted disruption of the class B scavenger receptor CD36 protects against atherosclerotic lesion development in mice. J Clin Invest. 2000; 105:1049–1056. [PubMed: 10772649]
16. Moore KJ, Freeman MW. Scavenger receptors in atherosclerosis: beyond lipid uptake. Arterioscler Thromb Vasc Biol. 2006; 26:1702–1711. [PubMed: 16728653]
17. Seimon TA, Nadolski MJ, Liao X, Magallon J, Nguyen M, Feric NT, Koschinsky ML, Harkewicz R, Witztum JL, Tsimikas S, Golenbock D, Moore KJ, Tabas I. Atherogenic lipids and lipoproteins trigger CD36-TLR2-dependent apoptosis in macrophages undergoing endoplasmic reticulum stress. Cell Metab. 2010; 12:467–482. [PubMed: 21035758]
18. Turner WW, Hartvigsen K, Boullier A, Montano EN, Witztum JL, VanNieuwenhze MS. Design and synthesis of a stable oxidized phospholipid mimic with specific binding recognition for macrophage scavenger receptors. J Med Chem. 2012; 55:8178–8182. [PubMed: 22934615]
19. Collot-Teixeira S, Martin J, McDermott-Roe C, Poston R, McGregor JL. CD36 and macrophages in atherosclerosis. Cardiovasc Res. 2007; 75:468–477. [PubMed: 17442283]
20. Curtiss LK. Reversing atherosclerosis? N Engl J Med. 2009; 360:1144–1146. [PubMed: 19279347]
21. Silverstein RL. Inflammation, atherosclerosis, and arterial thrombosis: role of the scavenger receptor CD36. Cleve Clin J Med. 2009; 76(Suppl 2):S27–30. [PubMed: 19376978]
22. Harb D, Bujold K, Febbraio M, Sirois MG, Ong H, Marleau S. The role of the scavenger receptor CD36 in regulating mononuclear phagocyte trafficking to atherosclerotic lesions and vascular inflammation. Cardiovasc Res. 2009; 83:42–51. [PubMed: 19264766]
23. Lipinski MJ, Frias JC, Amirbekian V, Briley-Saebo KC, Mani V, Samber D, Abbate A, Aguinaldo JG, Massey D, Fuster V, Vetrovec GW, Fayad ZA. Macrophage-specific lipid-based nanoparticles improve cardiac magnetic resonance detection and characterization of human atherosclerosis. JACC Cardiovasc Imaging. 2009; 2:637–647. [PubMed: 19442953]
24. Berliner JA, Leitinger N, Tsimikas S. The role of oxidized phospholipids in atherosclerosis. J Lipid Res. 2009; 50(Suppl):S207–212. [PubMed: 19059906]
25. Podrez EA, Poliakov E, Shen Z, Zhang R, Deng Y, Sun M, Finton PJ, Shan L, Gugiu B, Fox PL, Hoff HF, Salomon RG, Hazen SL. Identification of a novel family of oxidized phospholipids that serve as ligands for the macrophage scavenger receptor CD36. J Biol Chem. 2002; 277:38503–38516. [PubMed: 12105195]
26. Zhang L, Gu FX, Chan JM, Wang AZ, Langer RS, Farokhzad OC. Nanoparticles in medicine: therapeutic applications and developments. Clin Pharmacol Ther. 2008; 83:761–769. [PubMed: 17957183]
27. Peer D, Karp JM, Hong S, Farokhzad OC, Margalit R, Langer R. Nanocarriers as an emerging platform for cancer therapy. Nat Nanotechnol. 2007; 2:751–760. [PubMed: 18654426]

Author Manuscript Author Manuscript Author Manuscript Author Manuscript

28. Sima AV, Stancu CS, Simionescu M. Vascular endothelium in atherosclerosis. Cell Tissue Res. 2009; 335:191–203. [PubMed: 18797930]
29. Quillard T, Libby P. Molecular imaging of atherosclerosis for improving diagnostic and therapeutic development. Circ Res. 2012; 111:231–244. [PubMed: 22773426]
30. Wong C, Stylianopoulos T, Cui J, Martin J, Chauhan VP, Jiang W, Popovic Z, Jain RK, Bawendi MG, Fukumura D. Multistage nanoparticle delivery system for deep penetration into tumor tissue. Proc Natl Acad Sci U S A. 2011; 108:2426–2431. [PubMed: 21245339]
31. Wang S, Wu D, Matthan NR, Lamon-Fava S, Lecker JL, Lichtenstein AH. Reduction in dietary omega-6 polyunsaturated fatty acids: eicosapentaenoic acid plus docosahexaenoic acid ratio minimizes atherosclerotic lesion formation and inflammatory response in the LDL receptor null mouse. Atherosclerosis. 2009; 204:147–155. [PubMed: 18842266]
32. Havel RJ, Eder HA, Bragdon JH. The distribution and chemical composition of ultracentrifugally separated lipoproteins in human serum. J Clin Invest. 1955; 34:1345–1353. [PubMed: 13252080]
33. Han KH, Chang MK, Boullier A, Green SR, Li A, Glass CK, Quehenberger O. Oxidized LDL reduces monocyte CCR2 expression through pathways involving peroxisome proliferator-activated receptor gamma. J Clin Invest. 2000; 106:793–802. [PubMed: 10995790]
34. Zhang J, Nie S, Wang S. Nanoencapsulation enhances epigallocatechin-3-gallate stability and its antiatherogenic bioactivities in macrophages. J Agric Food Chem. 2013; 61:9200–9209. [PubMed: 24020822]
35. Duivenvoorden R, Tang J, Cormode DP, Mieszawska AJ, Izquierdo-Garcia D, Ozcan C, Otten MJ, Zaidi N, Lobatto ME, van Rijs SM, Priem B, Kuan EL, Martel C, Hewing B, Sager H, Nahrendorf M, Randolph GJ, Stroes ES, Fuster V, Fisher EA, Fayad ZA, Mulder WJ. A statin-loaded reconstituted high-density lipoprotein nanoparticle inhibits atherosclerotic plaque inflammation. Nat Commun. 2014; 5:3065. [PubMed: 24445279]
36. Gabizon A, Papahadjopoulos D. Liposome formulations with prolonged circulation time in blood and enhanced uptake by tumors. Proc Natl Acad Sci U S A. 1988; 85:6949–6953. [PubMed: 3413128]
37. Sosnovik DE, Nahrendorf M, Deliolanis N, Novikov M, Aikawa E, Josephson L, Rosenzweig A, Weissleder R, Ntziachristos V. Fluorescence tomography and magnetic resonance imaging of myocardial macrophage infiltration in infarcted myocardium in vivo. Circulation. 2007; 115:1384–1391. [PubMed: 17339546]
38. Libby P. Inflammation in atherosclerosis. Arterioscler Thromb Vasc Biol. 2012; 32:2045–2051. [PubMed: 22895665]
39. Tang TY, Howarth SP, Miller SR, Graves MJ, Patterson AJ, JMUK-I, Li ZY, Walsh SR, Brown AP, Kirkpatrick PJ, Warburton EA, Hayes PD, Varty K, Boyle JR, Gaunt ME, Zalewski A, Gillard JH. The ATHEROMA (Atorvastatin Therapy: Effects on Reduction of Macrophage Activity) Study. Evaluation using ultrasmall superparamagnetic iron oxide-enhanced magnetic resonance imaging in carotid disease. J Am Coll Cardiol. 2009; 53:2039–2050. [PubMed: 19477353]
40. Hyafil F, Cornily JC, Feig JE, Gordon R, Vucic E, Amirbekian V, Fisher EA, Fuster V, Feldman LJ, Fayad ZA. Noninvasive detection of macrophages using a nanoparticulate contrast agent for computed tomography. Nat Med. 2007; 13:636–641. [PubMed: 17417649]
41. Libby P, Sasiela W. Plaque stabilization: Can we turn theory into evidence? Am J Cardiol. 2006; 98:26P–33P.
42. Jaffer FA, Libby P, Weissleder R. Optical and multimodality molecular imaging: insights into atherosclerosis. Arterioscler Thromb Vasc Biol. 2009; 29:1017–1024. [PubMed: 19359659]
43. Naghavi M, Libby P, Falk E, Casscells SW, Litovsky S, Rumberger J, Badimon JJ, Stefanadis C, Moreno P, Pasterkamp G, Fayad Z, Stone PH, Waxman S, Raggi P, Madjid M, Zarrabi A, Burke A, Yuan C, Fitzgerald PJ, Siscovick DS, de Korte CL, Aikawa M, Airaksinen KE, Assmann G, Becker CR, Chesebro JH, Farb A, Galis ZS, Jackson C, Jang IK, Koenig W, Lodder RA, March K, Demirovic J, Navab M, Priori SG, Rekhter MD, Bahr R, Grundy SM, Mehran R, Colombo A, Boerwinkle E, Ballantyne C, Insull W Jr, Schwartz RS, Vogel R, Serruys PW, Hansson GK, Faxon DP, Kaul S, Drexler H, Greenland P, Muller JE, Virmani R, Ridker PM, Zipes DP, Shah PK, Willerson JT. From vulnerable plaque to vulnerable patient: a call for new definitions and risk assessment strategies: Part II. Circulation. 2003; 108:1772–1778. [PubMed: 14557340]

Author Manuscript Author Manuscript Author Manuscript Author Manuscript

44. Terpstra V, Bird DA, Steinberg D. Evidence that the lipid moiety of oxidized low density lipoprotein plays a role in its interaction with macrophage receptors. Proc Natl Acad Sci U S A. 1998; 95:1806–1811. [PubMed: 9465098]
45. Bird DA, Gillotte KL, Horkko S, Friedman P, Dennis EA, Witztum JL, Steinberg D. Receptors for oxidized low-density lipoprotein on elicited mouse peritoneal macrophages can recognize both the modified lipid moieties and the modified protein moieties: implications with respect to macrophage recognition of apoptotic cells. Proc Natl Acad Sci U S A. 1999; 96:6347–6352. [PubMed: 10339590]
46. Podrez EA, Poliakov E, Shen Z, Zhang R, Deng Y, Sun M, Finton PJ, Shan L, Febbraio M, Hajjar DP, Silverstein RL, Hoff HF, Salomon RG, Hazen SL. A novel family of atherogenic oxidized phospholipids promotes macrophage foam cell formation via the scavenger receptor CD36 and is enriched in atherosclerotic lesions. J Biol Chem. 2002; 277:38517–38523. [PubMed: 12145296]
47. Rahaman SO, Lennon DJ, Febbraio M, Podrez EA, Hazen SL, Silverstein RL. A CD36-dependent signaling cascade is necessary for macrophage foam cell formation. Cell Metab. 2006; 4:211–221. [PubMed: 16950138]
48. Greenberg ME, Li XM, Gugiu BG, Gu X, Qin J, Salomon RG, Hazen SL. The lipid whisker model of the structure of oxidized cell membranes. J Biol Chem. 2008; 283:2385–2396. [PubMed: 18045864]
49. Kar NS, Ashraf MZ, Valiyaveettil M, Podrez EA. Mapping and characterization of the binding site for specific oxidized phospholipids and oxidized low density lipoprotein of scavenger receptor CD36. J Biol Chem. 2008; 283:8765–8771. [PubMed: 18245080]
50. Li XM, Salomon RG, Qin J, Hazen SL. Conformation of an endogenous ligand in a membrane bilayer for the macrophage scavenger receptor CD36. Biochemistry. 2007; 46:5009–5017. [PubMed: 17407326]
51. Kooi ME, Cappendijk VC, Cleutjens KB, Kessels AG, Kitslaar PJ, Borgers M, Frederik PM, Daemen MJ, van Engelshoven JM. Accumulation of ultrasmall superparamagnetic particles of iron oxide in human atherosclerotic plaques can be detected by in vivo magnetic resonance imaging. Circulation. 2003; 107:2453–2458. [PubMed: 12719280]
52. Amirbekian V, Lipinski MJ, Briley-Saebo KC, Amirbekian S, Aguinaldo JG, Weinreb DB, Vucic E, Frias JC, Hyafil F, Mani V, Fisher EA, Fayad ZA. Detecting and assessing macrophages in vivo to evaluate atherosclerosis noninvasively using molecular MRI. Proc Natl Acad Sci U S A. 2007; 104:961–966. [PubMed: 17215360]
53. Skajaa T, Cormode DP, Falk E, Mulder WJ, Fisher EA, Fayad ZA. High-density lipoprotein-based contrast agents for multimodal imaging of atherosclerosis. Arterioscler Thromb Vasc Biol. 2010; 30:169–176. [PubMed: 19815819]
54. Cormode DP, Jarzyna PA, Mulder WJ, Fayad ZA. Modified natural nanoparticles as contrast agents for medical imaging. Adv Drug Deliv Rev. 2010; 62:329–338. [PubMed: 19900496]
55. Magnoni M, Ammirati E, Camici PG. Non-invasive molecular imaging of vulnerable atherosclerotic plaques. J Cardiol. 2015; 65:261–269. [PubMed: 25702846]
56. Kamaly N, Fredman G, Subramanian M, Gadde S, Pesic A, Cheung L, Fayad ZA, Langer R, Tabas I, Farokhzad OC. Development and in vivo efficacy of targeted polymeric inflammation-resolving nanoparticles. Proc Natl Acad Sci U S A. 2013; 110:6506–6511. [PubMed: 23533277]
57. Fredman G, Kamaly N, Spolitu S, Milton J, Ghorpade D, Chiasson R, Kuriakose G, Perretti M, Farokhzad O, Tabas I. Targeted nanoparticles containing the proresolving peptide Ac2-26 protect against advanced atherosclerosis in hypercholesterolemic mice. Sci Transl Med. 2015; 7:275ra220.
58. Rose RA, Giles WR. Natriuretic peptide C receptor signalling in the heart and vasculature. J Physiol. 2008; 586:353–366. [PubMed: 18006579]
59. Liu Y, Abendschein D, Woodard GE, Rossin R, McCommis K, Zheng J, Welch MJ, Woodard PK. Molecular imaging of atherosclerotic plaque with (64)Cu-labeled natriuretic peptide and PET. J Nucl Med. 2010; 51:85–91. [PubMed: 20008978]
60. Palekar RU, Jallouk AP, Lanza GM, Pan H, Wickline SA. Molecular imaging of atherosclerosis with nanoparticle-based fluorinated MRI contrast agents. Nanomedicine (Lond). 2015; 10:1817–1832. [PubMed: 26080701]

Author Manuscript Author Manuscript Author Manuscript Author Manuscript

61. Leuschner F, Nahrendorf M. Molecular imaging of coronary atherosclerosis and myocardial infarction: considerations for the bench and perspectives for the clinic. Circ Res. 2011; 108:593–606. [PubMed: 21372291]

62. Weissleder R, Nahrendorf M, Pittet MJ. Imaging macrophages with nanoparticles. Nat Mater. 2014; 13:125–138. [PubMed: 24452356]

63. Wildgruber M, Swirski FK, Zernecke A. Molecular imaging of inflammation in atherosclerosis. Theranostics. 2013; 3:865–884. [PubMed: 24312156]

64. Mulder WJ, Jaffer FA, Fayad ZA, Nahrendorf M. Imaging and nanomedicine in inflammatory atherosclerosis. Sci Transl Med. 2014; 6:239sr231.

Author Manuscript Author Manuscript Author Manuscript Author Manuscript

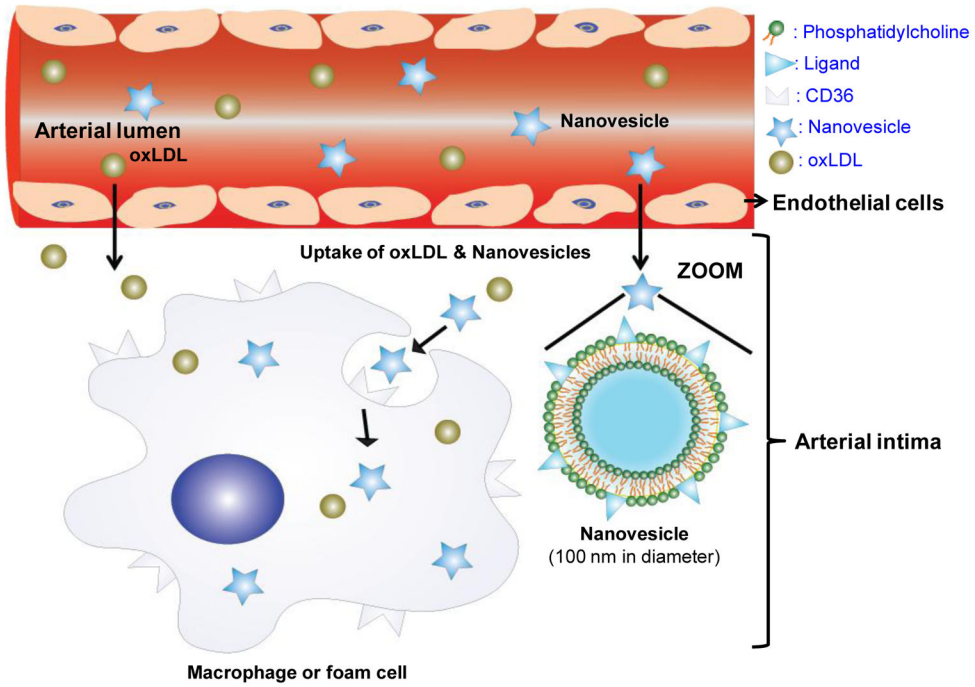

Fig. 1.

Illustration of CD36-targeted nanovesicle composition, structure and targeting mechanisms to intimal macrophages. Targeted nanovesicles in the circulation system migrate into the arterial intimal layer, and then target to intimal macrophages via binding to their CD36 receptors.

Author Manuscript Author Manuscript Author Manuscript Author Manuscript

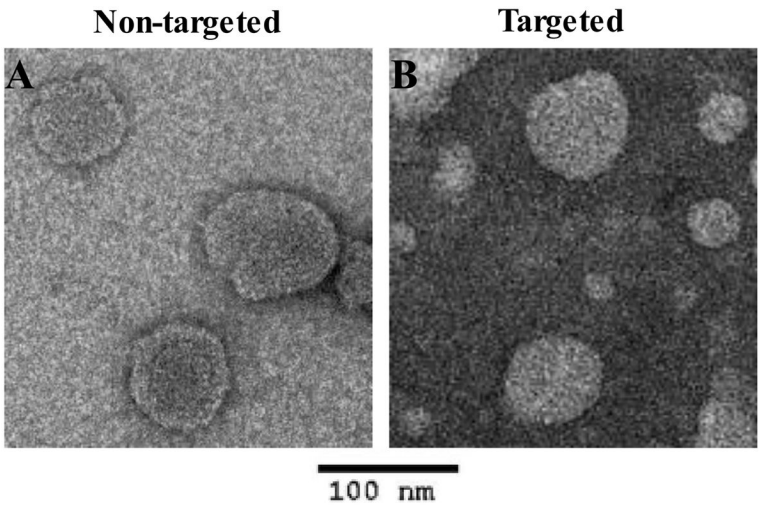

Fig. 2.

Transmission electron microscope (TEM) images of non-targeted nanovesicles (A) and targeted nanovesicles (B) stained by 2% of uranyl acetate.

Author Manuscript Author Manuscript Author Manuscript Author Manuscript

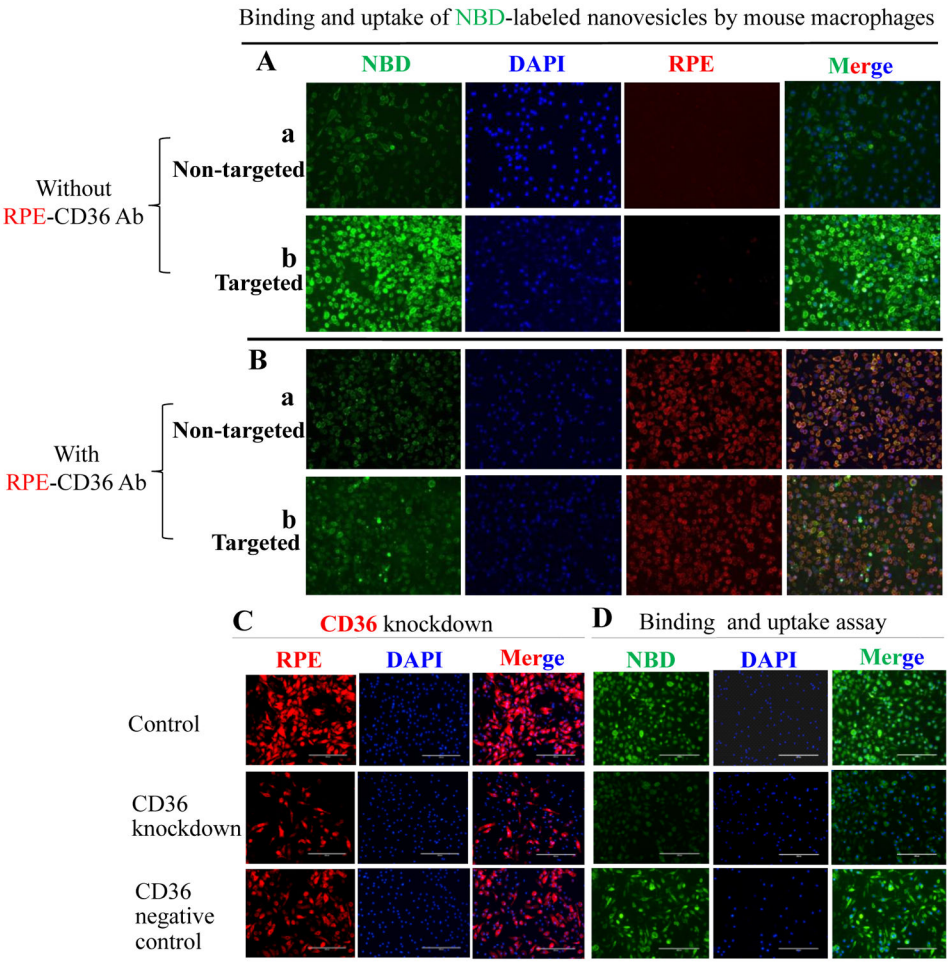

Fig. 3.

The binding and uptake of NBD-labeled nanovesicles by mouse peritoneal macrophages. A, Mouse peritoneal macrophages were treated with non-targeted nanovesicles (a) or targeted nanovesicles (b); B, Mouse peritoneal macrophages were treated with RPE-labeled anti-mouse CD36 antibody (λ of excitation is 496 nm, λ of emission is 578 nm) in combination with non-targeted nanovesicles (a) or targeted nanovesicles (b). Targeted nanovesicles bind to mouse macrophages via CD36 receptors. C, Mouse peritoneal macrophages were transfected without (control) or with CD36 siRNA (CD36 knockdown) or scramble siRNA (negative control). CD36 siRNA transfection decreased CD36 protein expression in mouse peritoneal macrophages; D, The binding and uptake of targeted nanovesicles by control, CD36 knockdown, or CD36 negative control mouse peritoneal macrophages. Bar length is 200 μm. NBD-labeled nanovesicles were green (λ of excitation is 460 nm; λ of emission is 535 nm). Cell nuclei were stained by DAPI (λ of excitation is 358 nm, λ of emission is 461 nm) (blue color). Images are representatives of three independent experiments.

Author Manuscript Author Manuscript Author Manuscript Author Manuscript

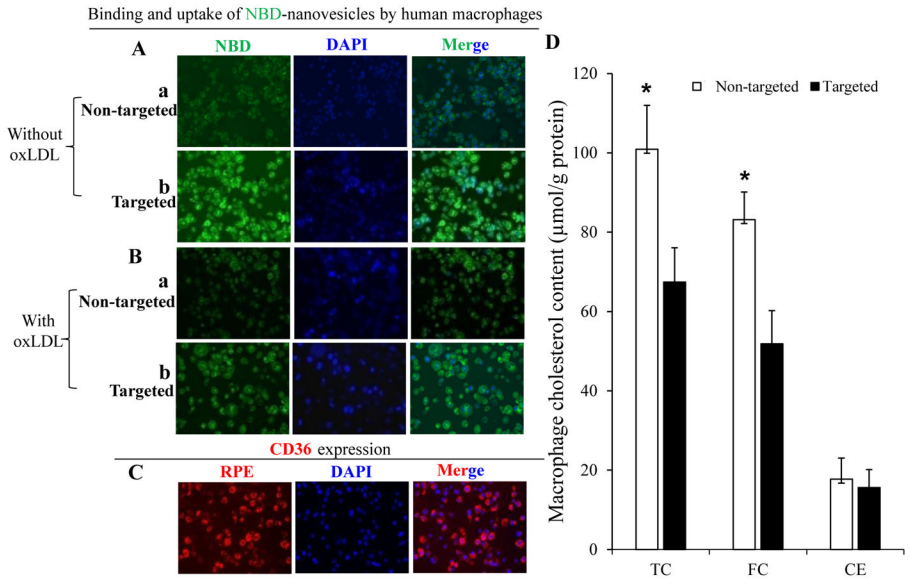

Fig. 4.

The binding and uptake of NBD-labeled nanovesicles by THP-1 derived macrophages. A, THP-1 derived macrophages were treated with non-targeted nanovesicles (a) or targeted nanovesicles (b); B, Co-incubation of human minimally oxLDL with either non-targeted nanovesicles (a) or targeted nanovesicles (b); C, CD36 protein expression was confirmed using RPE-labeled anti-CD36 antibody; D, THP-1 derived macrophages were pre-treated with non-targeted or targeted nanovesicles for 30 minutes, then incubated with 40 μg/mL of human minimally oxLDL for additional 1.5 hours. Cholesterol content in those macrophages was determined using a HPLC system. Data are calculated from three independent experiments and expressed as means ± SD, * indicates $p<0.05$.

Author Manuscript Author Manuscript Author Manuscript Author Manuscript

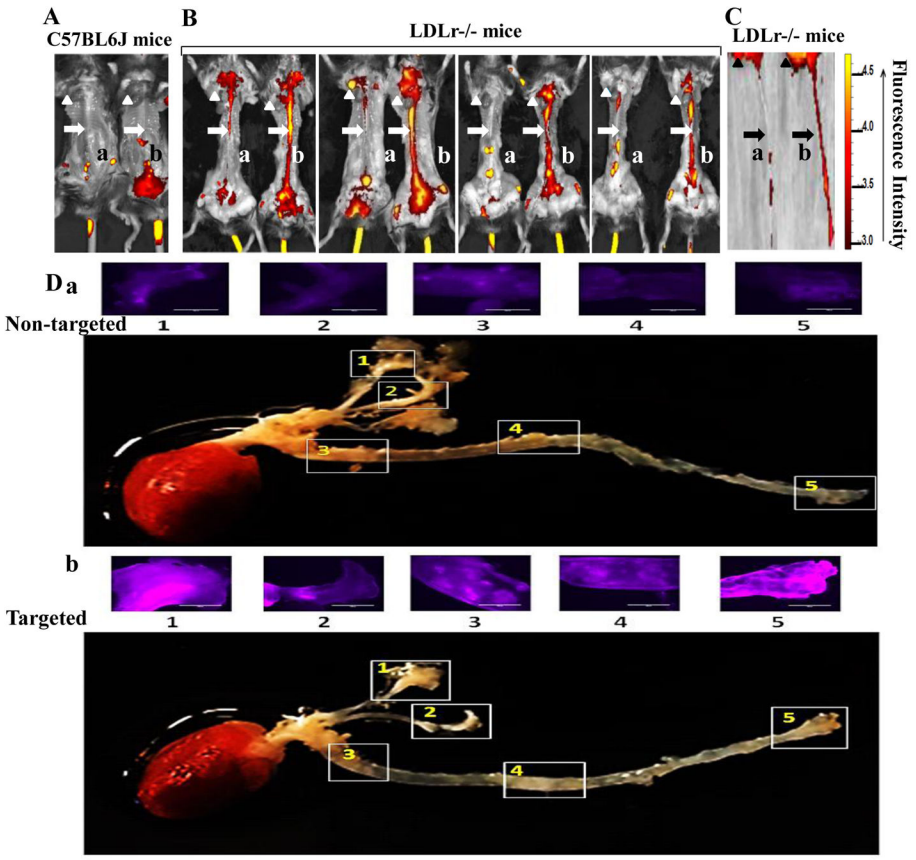

Fig. 5.

Target specificity of DiR-labeled nanovesicles to atherosclerotic lesions in mice. A&B, *In vivo* images of one pair of C57BL6J mice (A) and 4 pairs of LDLr−/− mice (B) intravenously injected with DiR-labeled non-targeted nanovesicles (a) or DiR-labeled targeted nanovesicles (b) using an IVIS® Lumina XR imaging system; Arrow heads denote hearts, and arrows denote aortas. The liver, spleen, kidneys, and additional abdominal organs and tissues were removed for better imaging of aortas. C, Representative images of hearts and aortas isolated from the 4th pair of LDLr−/− mice in the panel B using an IVIS® Lumina XR imaging system; D, Representative images of DiR signals on the inner surface of five lesion areas on the longitudinally opened aortas isolated from the 2nd pair of LDLr−/− mice in panel B using an EvoS Auto fluorescence microscope. Bar length is 1000 μm. (N=4 for each group).

Author Manuscript Author Manuscript Author Manuscript Author Manuscript

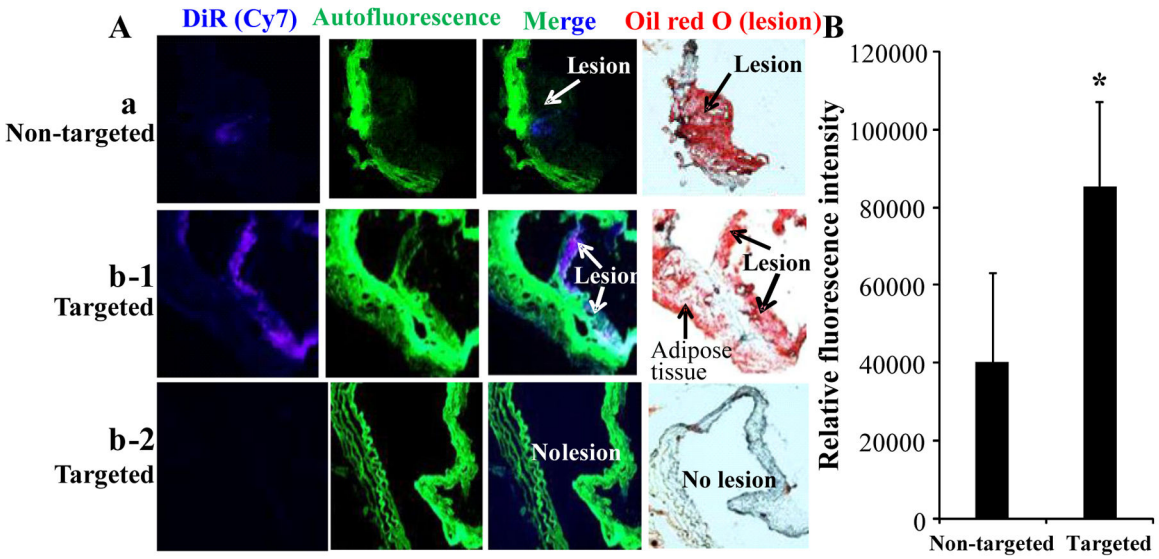

Fig. 6.

Target specificity of DiR-labeled nanovesicles to atherosclerotic lesions in cross-sections of aortas in mice. A, Representative images from the atherosclerotic lesions of cross-sections in LDLr−/− mice and aortic non-lesion areas in C57BL6J mice. Fig. 6A-a and 6A-b-1 were obtained from LDLr−/− mice intravenously injected with DiR-labeled non-targeted nanovesicles (a) or DiR-labeled targeted nanovesicles (b-1), respectively. Fig. 6A-b-2 was obtained from C57BL6J mice intravenously injected with DiR-labeled targeted nanovesicles. (N=4 for each group). B, Relative Cy7 signal intensity in the cross-sections of arteries isolated from LDLr−/− mice intravenously injected with DiR-labeled non-targeted nanovesicles or DiR-labeled targeted nanovesicles was calculated using the NIH ImageJ software. Values are the means of relative Cy7 signal intensity of cross-sections of aortas, with standard deviations represented by vertical bars. * indicates $p<0.05$.

Author Manuscript Author Manuscript Author Manuscript Author Manuscript

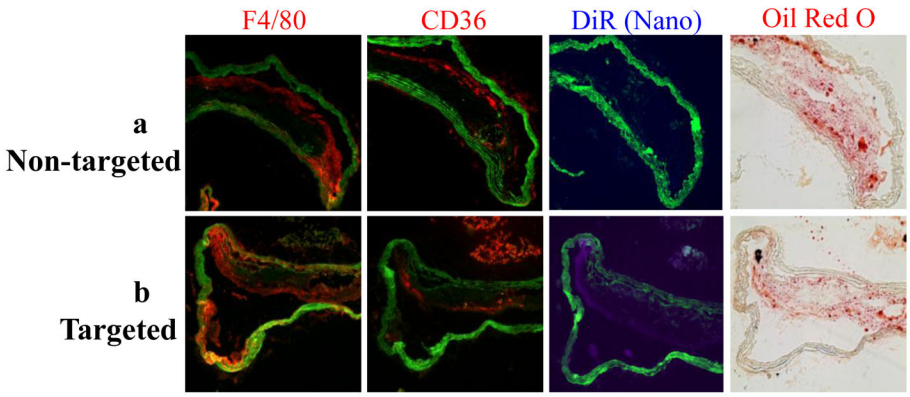

Fig. 7.

Nanovesicles carrying KOdiA-PC on their surface target to atherosclerotic lesions through binding to CD36 receptors of intimal macrophages. Targeted nanovesicles overlay with F4/80 and CD36 receptors stained by immunohistochemistry in cross-sections of aortas isolated from LDLr−/− mice, which were intravenously injected with nanovesicles without (a) or with (b) the target ligand, KOdiA-PC. Images are representative of cross-sections of aortas isolated from four mice in each group.

Author Manuscript

Author Manuscript

Author Manuscript

Author Manuscript

Table 1

Particle size, zeta potential and polydispersity index of nanovesicles

Characteristics	Non-targeted nanovesicles	Targeted nanovesicles
Particle size (nm)	100.6 ± 1.3	100.8 ± 0.9
Zeta potential (mV)	−22.78 ± 7.3	−20.1 ± 4.6
Polydispersity index	0.09 ± 0.01	0.11 ± 0.06